PROCEEDINGS OF SPIE

SPIEDigitalLibrary.org/conference-proceedings-of-spie

Development of a variable structure-based fault detection and diagnosis strategy applied to an electromechanical system

S. Andrew Gadsden, T. Kirubarajan

SPIE.

Development of a Variable Structure-Based Fault Detection and Diagnosis Strategy Applied to an Electromechanical System

S. Andrew Gadsden[1] and T. (Kiruba) Kirubarajan[2]
1 University of Guelph, Guelph, Ontario, Canada, N1G 2W1;
2 McMaster University, Hamilton, Ontario, Canada, L8S 4L7

ABSTRACT

Signal processing techniques are prevalent in a wide range of fields: control, target tracking, telecommunications, robotics, fault detection and diagnosis, and even stock market analysis, to name a few. Although first introduced in the 1950s, the most popular method used for signal processing and state estimation remains the Kalman filter (KF). The KF offers an optimal solution to the estimation problem under strict assumptions. Since this time, a number of other estimation strategies and filters were introduced to overcome robustness issues, such as the smooth variable structure filter (SVSF). In this paper, properties of the SVSF are explored in an effort to detect and diagnosis faults in an electromechanical system. The results are compared with the KF method, and future work is discussed.

Keywords: Variable structure systems, estimation theory, signal processing, fault detection and diagnosis

1. INTRODUCTION

Control of an engineering system depends on how well the system states and parameters are known. Observations and measurements of the system are made through the use of sensors, however this data often contains unwanted signals, noise, and disturbances. Filters are used to remove unwanted components in an effort to provide an accurate estimate of the states [1]. Although it is well over 50 years old, the most common and well-studied estimation method remains the Kalman filter (KF) [2, 3]. The KF yields a statistically optimal solution for linear estimation problems, as defined by (1.1) and (1.2), in the presence of Gaussian noise where $P(w_k)\sim\mathcal{N}(0,Q_k)$ and $P(v_k)\sim\mathcal{N}(0,R_k)$, and under the assumption that the system and measurement dynamics are known. A typical model is represented by the following equations:

$$x_{k+1} = Ax_k + Bu_k + w_k \tag{1.1}$$

$$z_{k+1} = Cx_{k+1} + v_{k+1} \tag{1.2}$$

where x refers to the state vector, A is the system matrix (dynamics), B is the input gain matrix, u is the system input, z is the measurement vector, C is the measurement matrix, w is the system noise vector, v is the measurement noise vector, and k refers to the time step.

It is the goal of any filter to remove the effects that the system w_k and measurement v_k noise have on extracting the true state values x_k from the measurements z_k. The KF is formulated in a predictor-corrector manner. The states are first estimated using the system model, termed as a priori estimates, meaning 'prior to' knowledge of the observations. A correction term is then added based on the innovation (also called residuals or measurement errors), thus forming the updated or a posteriori (meaning 'subsequent to' the observations) state estimates. The KF correction term or gain is derived by taking the partial derivative of the trace of the state error covariance matrix with respect to the gain, setting the equation to zero, and then solving for the gain. The optimality of the KF comes at a price of stability and robustness. The KF assumes that the system model is known and linear, the system and measurement noises are white, and the states have initial conditions with known means and variances [4, 5]. However, the previous assumptions do not always hold in real applications. If these assumptions are violated, the KF yields suboptimal results and can become unstable [6]. Furthermore, the KF is sensitive to computer precision and

Signal Processing, Sensor/Information Fusion, and Target Recognition XXVI, edited by Ivan Kadar, Proc. of SPIE Vol. 10200, 102001E · © 2017 SPIE · CCC code: 0277-786X/17/$18 · doi: 10.1117/12.2262570

the complexity of computations involving matrix inversions [7]. In an effort to further increase stability, the KF has been combined with a variety of square root algorithms and methods, such as Cholesky decomposition, UD-factorization, and triangularization algorithms [8, 9, 10, 11]. These methods are based on reformulating the KF equations by using numerically stable implementations to mathematically increase the arithmetic precision of the computation [7]. Increasing the arithmetic precision reduces the effects of round-off errors, which improves the overall numerical stability of the filter.

Variable structure-based estimation methods have been introduced over the past few decades, and offer an alternative to the KF with improved robustness and stability to modeling uncertainties and disturbances [12]. However, it is important to note that these methods are sub-optimal in terms of estimation accuracy. Variable structure system theory originated from the Soviet Union in the 1940s [13, 14]. A special subcategory of it referred to as sliding mode control (SMC) is commonly used in control applications as it provides enhanced robustness and stability. In a typical sliding mode controller, a discontinuous switching gain is used to maintain the states along some desired trajectory [14]. The discontinuous gain is determined based on the distance of the states from a switching hyperplane. The gain forces the states to convergence onto the hyperplane, and slide along it [15]. While on the hyperplane and under ideal conditions, the state trajectory becomes insensitive to disturbances and uncertainties. The discontinuous switching brings an inherent amount of stability to the control strategy. A number of sliding mode observers and filters have been proposed in literature [16, 17].

This paper proposes the use of a variable structure-based estimation method, referred to the smooth variable structure filter (SVSF), in an effort to detect and identify changes or faults experienced by an electromechanical system. In Section 2, the basic KF and SVSF equations are presented. The proposed fault detection and diagnosis strategy is presented in Section 3. The electromechanical system is presented in Section 4, and the results are discussed in detail. The paper concludes and future work is proposed in the final section.

2. ESTIMATION THEORIES

Kalman Filter

The KF has been broadly applied to problems covering state and parameter estimation, signal processing, target tracking, fault detection and diagnosis, and even financial analysis [18, 19]. The success of the KF comes from the optimality of the Kalman gain in minimizing the trace of the a posteriori state error covariance matrix [20, 21]. The trace is taken because it represents the state error vector in the estimation process [22]. The following five equations form the core of the KF algorithm, and are used in an iterative fashion. Equations (2.1) and (2.2) define the a priori state estimate $\hat{x}_{k+1|k}$ and the corresponding state error covariance matrix $P_{k+1|k}$, respectively.

$$\hat{x}_{k+1|k} = A\hat{x}_{k|k} + Bu_k \tag{2.1}$$

$$P_{k+1|k} = AP_{k|k}A^T + Q_k \tag{2.2}$$

The Kalman gain K_{k+1} (2.3) is used to update the state estimate $\hat{x}_{k+1|k+1}$ as per (2.4). The gain makes use of an innovation covariance S_{k+1}, which is defined as the inverse term found in (2.3).

$$K_{k+1} = P_{k+1|k}C^T\left[CP_{k+1|k}C^T + R_{k+1}\right]^{-1} \tag{2.3}$$

$$\hat{x}_{k+1|k+1} = \hat{x}_{k+1|k} + K_{k+1}\left[z_{k+1} - C\hat{x}_{k+1|k}\right] \tag{2.4}$$

The a posteriori state error covariance matrix $P_{k+1|k+1}$ is then calculated (2.5), and is used iteratively, as per (2.2).

$$P_{k+1|k+1} = [I - K_{k+1}C]P_{k+1|k}[I - K_{k+1}C]^T + K_{k+1}R_{k+1}K_{k+1}^T \tag{2.5}$$

A number of different methods have extended the classical KF to nonlinear systems, with the most popular and simplest method being the extended Kalman filter (EKF) [4, 23]. The EKF is conceptually similar to the KF; however, the nonlinear system is linearized according to its Jacobian. This linearization process introduces uncertainties that can cause numerical instability and inaccurate estimates [23].

Smooth Variable Structure Filter

When given an upper bound on the level of unmodeled dynamics and noise, the SVSF is stable and robust to modeling uncertainties, noise, and disturbances [24, 25, 26]. The SVSF method is model-based and may be applied to differentiable linear or nonlinear dynamic equations [27, 28]. The basic estimation concept of the SVSF is shown in Fig. 1.

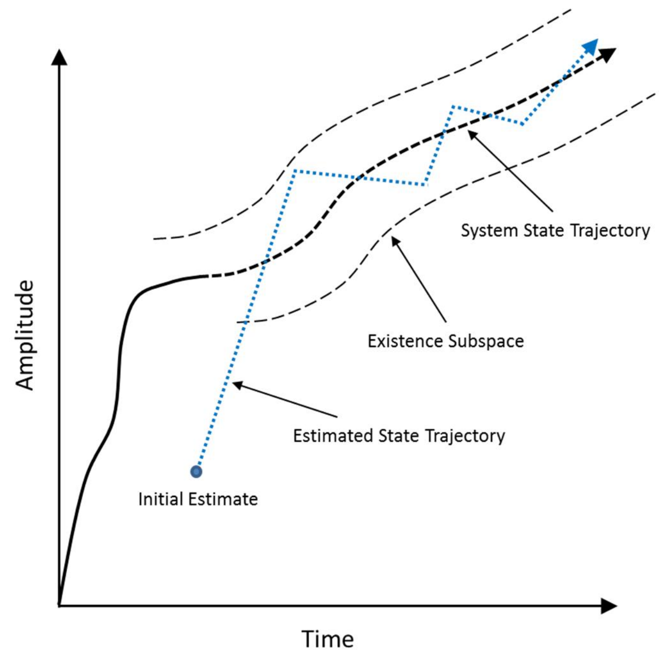

Figure 1. Standard SVSF estimation concept [20].

The SVSF estimation process is similar to the KF, with the main exception being the gain calculation [29]. The predicted state estimates $\hat{x}_{k+1|k}$ and state error covariance $P_{k+1|k}$ are first calculated as per (2.1) and (2.2). Utilizing the predicted state estimates $\hat{x}_{k+1|k}$, the corresponding predicted measurements $\hat{z}_{k+1|k}$ and measurement errors $e_{z,k+1|k}$ may be calculated:

$$\hat{z}_{k+1|k} = C\hat{x}_{k+1|k} \tag{2.6}$$

$$e_{z,k+1|k} = z_{k+1} - \hat{z}_{k+1|k} \tag{2.7}$$

The SVSF gain is a function of: the a priori and the a posteriori measurement errors $e_{z,k+1|k}$ and $e_{z,k|k}$; the smoothing boundary layer widths ψ; and the 'SVSF' memory or convergence rate γ. The SVSF gain K_{k+1} is defined as follows [20, 30]:

$$K_{k+1} = C_k^{+} diag\left[\left(\left|e_{z_{k+1|k}}\right| + \gamma\left|e_{z_{k|k}}\right|\right) \circ sat\left(\bar{\psi}^{-1} e_{z_{k+1|k}}\right)\right] diag\left(e_{z_{k+1|k}}\right)^{-1} \tag{2.8}$$

where $\circ$ signifies Schur (or element-by-element) multiplication and the superscript $+$ refers to the pseudoinverse of a matrix. The saturation function of (2.8) is defined by the following:

$$sat\left(\bar{\psi}^{-1}e_{z_{k+1|k}}\right) = \begin{cases} 1, & e_{z_i,k+1|k}/\psi_i \geq 1 \\ e_{z_i,k+1|k}/\psi_i, & -1 < e_{z_i,k+1|k}/\psi_i < 1 \\ -1, & e_{z_i,k+1|k}/\psi_i \leq -1 \end{cases} \tag{2.9}$$

where $\bar{\psi}^{-1}$ is a diagonal matrix constructed from the elements of the smoothing boundary layer vector ψ:

$$\bar{\psi}^{-1} = \begin{bmatrix} \frac{1}{\psi_1} & 0 & 0 \\ 0 & \ddots & 0 \\ 0 & 0 & \frac{1}{\psi_m} \end{bmatrix} \tag{2.10}$$

The state estimates $\hat{x}_{k+1|k}$ and state error covariance matrix $P_{k+1|k}$ are updated respectively as per (2.4) and (2.5). Finally, the updated measurement estimate $\hat{z}_{k+1|k+1}$ and measurement errors $e_{z,k+1|k+1}$ are calculated, and are used in later iterations:

$$\hat{z}_{k+1|k+1} = C\hat{x}_{k+1|k+1} \tag{2.11}$$

$$e_{z,k+1|k+1} = z_{k+1} - \hat{z}_{k+1|k+1} \tag{2.12}$$

The existence subspace shown in Fig. 1 represents the amount of uncertainties present in the estimation process, in terms of modeling errors or the presence of noise. The width of the existence space β is a function of the uncertain dynamics associated with the inaccuracy of the internal model of the filter as well as the measurement model, and varies with time [30]. Typically this value is not exactly known but an upper bound may be selected based on a priori knowledge. When the smoothing boundary layer is defined larger than the existence subspace boundary, the estimated state trajectory is smoothed. However, when the smoothing term is too small, chattering remains due to the uncertainties being underestimated.

3. PROPOSED FAULT DETECTION AND DIAGNOSIS STRATEGY

The partial derivative of the a posteriori covariance (trace) with respect to the smoothing boundary layer term ψ_{k+1} is the basis for obtaining a time-varying strategy for the specification of ψ_{k+1}. In linear systems, this smoothing boundary layer yields an optimal gain (exactly the KF) [20]. Previous forms of the SVSF included a vector form of ψ, which had a single smoothing boundary layer term for each corresponding measurement error [30]. Essentially, the boundary layer terms were independent of each other such that the measurement errors would not mix when calculating the corresponding gain, leading to reduced estimation accuracy. In an effort to obtain a smoothing boundary layer equation that yielded more accurate state estimates, a full smoothing boundary layer matrix was proposed in [20, 31]. Hence, consider the following smoothing boundary layer form:

$$\psi = \begin{bmatrix} \psi_{11} & \psi_{12} & \cdots & \psi_{1m} \\ \psi_{12} & \psi_{22} & \cdots & \psi_{2m} \\ \vdots & \vdots & \ddots & \vdots \\ \psi_{m1} & \psi_{m2} & \cdots & \psi_{mm} \end{bmatrix} \tag{3.1}$$

This definition includes terms that relate one smoothing boundary layer to another (i.e., off-diagonal terms). To solve for the time-varying smoothing boundary layer based on (3.1), consider the following in conjunction with (2.5):

$$\frac{\partial\left(trace[P_{k+1|k+1}]\right)}{\partial\psi} = 0 \tag{3.2}$$

As described in [32], a solution for the smoothing boundary layer from (3.2) is defined as follows:

$$\psi_{k+1} = \left(\bar{E}^{-1} C_k P_{k+1|k} C_k^T S_{k+1}^{-1}\right)^{-1} \tag{3.3}$$

where S_{k+1} and A are defined respectively by:

$$S_{k+1} = C_k P_{k+1} C_k^T + R_{k+1} \tag{3.4}$$

$$E = \left(\left|e_{z_{k+1|k}}\right| + \gamma \left|e_{z_{k|k}}\right|\right) \tag{3.5}$$

This paper proposes the use of (3.3) to determine the presence of modeling uncertainty which can be detected and identified as faults. For example, as discussed previously, the width of the smoothing boundary layer provides an indicator of performance in terms of the estimation accuracy. If the width or value is small, the system used by the SVSF closely matches that of the true system. Whereas if the width is large, the system used by the SVSF does not match the true system. If a finite number of system operations or models are known, then a bank of filters can be implemented and (3.3) can be used to accurately and quickly detect and identify the correct mode of operation. This concept is illustrated in Section 4.

4. ELECTROMECHANICAL SYSTEM AND SIMULATION RESULTS

Electromechanical System

In this paper, an electromechanical system based on a type of aerospace actuator was studied [33]. An electrohydrostatic actuator (EHA) is typically used in the aerospace industry for aircraft maneuvering by controlling flight surfaces. EHAs are self-contained units comprised of their own pump, hydraulic circuit, and actuating cylinder [30]. The main components of an EHA include a variable speed motor, an external gear pump, an accumulator, inner circuitry check valves, a cylinder (or actuator), and a bi-directional pressure relief mechanism. A mathematical model for the EHA has been described in detail in [34, 20]. For the purposes of this paper, only the main state space equations will be explored. The input to the system is the rotational speed of the pump ω_p, with typical units of rad/s. In this setup, the sample rate for this simulation was defined as $T = 0.1\ ms$. The state space equations are defined as follows:

$$x_{1,k+1} = x_{1,k} + T x_{2,k} + T w_{1,k} \tag{4.1}$$

$$x_{2,k+1} = x_{2,k} + T x_{3,k} + T w_{2,k} \tag{4.2}$$

$$\begin{aligned} x_{1,k+1} = {} & \left[1 - T\left(\frac{BV_0 + M\beta_e L}{MV_0}\right)\right] x_{3,k} - T\frac{(A^2 + BL)\beta_e}{MV_0} x_{2,k} \\ & - T\left[\frac{2B_2 V_0 x_{2,k} x_{3,k}}{MV_0} + \frac{\beta_e L\left(B_2 x_{2,k}^2 + B_0\right)}{MV_0}\right] sign(x_2, k) \\ & + T\frac{AD_p\beta_e}{MV_0} u_k + T w_{3,k} \end{aligned} \tag{4.3}$$

Note that A (in this case) refers to the piston cross-sectional area, $B_\#$ represents the load friction present in the system, β_e is the effective bulk modulus (i.e., the 'stiffness' in the hydraulic circuit), D_p refers to the pump displacement, L represents the leakage coefficient, M is the load mass (i.e., weight of the cylinders), and V_0 is the initial cylinder volume. The values used to obtain a linear normal operating model are summarized in the appendix. Two more models were created based on a severe friction fault (the friction was increased 3 times) and a severe leakage fault (the leakage coefficient was increased 4 times). The normal, friction fault, and leakage fault system matrices (A_1, A_2, and A_3) are respectively defined as follows:

$$A_1 = \begin{bmatrix} 1 & 0.0001 & 0 \\ 0 & 1 & 0.0001 \\ 0 & -41.0258 & 0.6099 \end{bmatrix} \tag{4.4}$$

$$A_2 = \begin{bmatrix} 1 & 0.0001 & 0 \\ 0 & 1 & 0.0001 \\ 0 & -51.8627 & 0.2226 \end{bmatrix} \tag{4.5}$$

$$A_3 = \begin{bmatrix} 1 & 0.0001 & 0 \\ 0 & 1 & 0.0001 \\ 0 & -73.5364 & 0.6015 \end{bmatrix} \tag{4.6}$$

Note that all three input gain matrices remained the same, and were calculated as follows:

$$B = \begin{bmatrix} 0 \\ 0 \\ 0.0135 \end{bmatrix} \tag{4.7}$$

Note also that artificial system and measurement noise was added to the simulation problem to make it more challenging. The zero-mean Gaussian noise was generated using system and measurement noise covariance's Q and R which were diagonal matrices with elements equal to 1×10^{-6}. The desired position, velocity, and acceleration trajectories are shown in the following three figures.

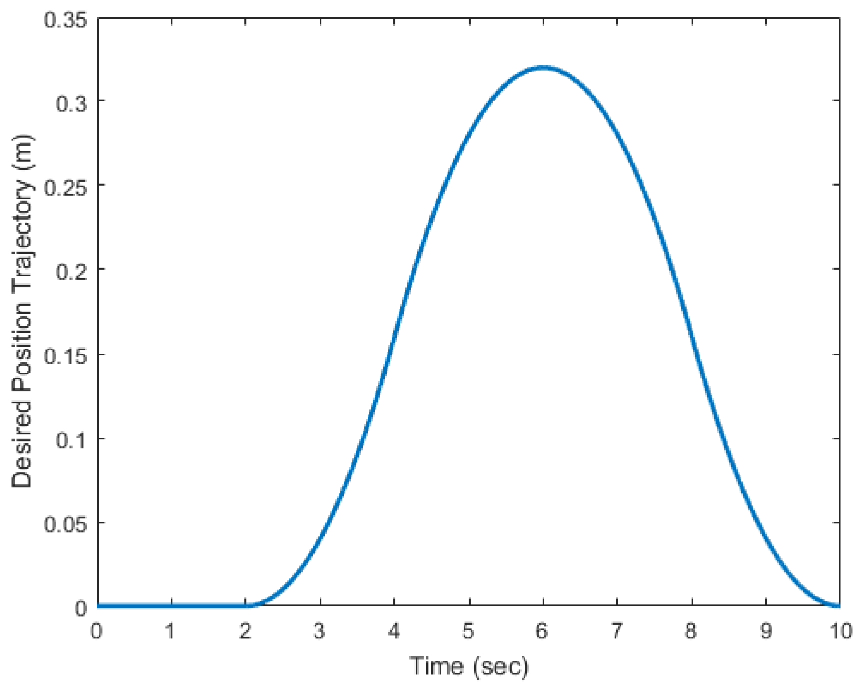

Figure 2. Desired EHA position trajectory.

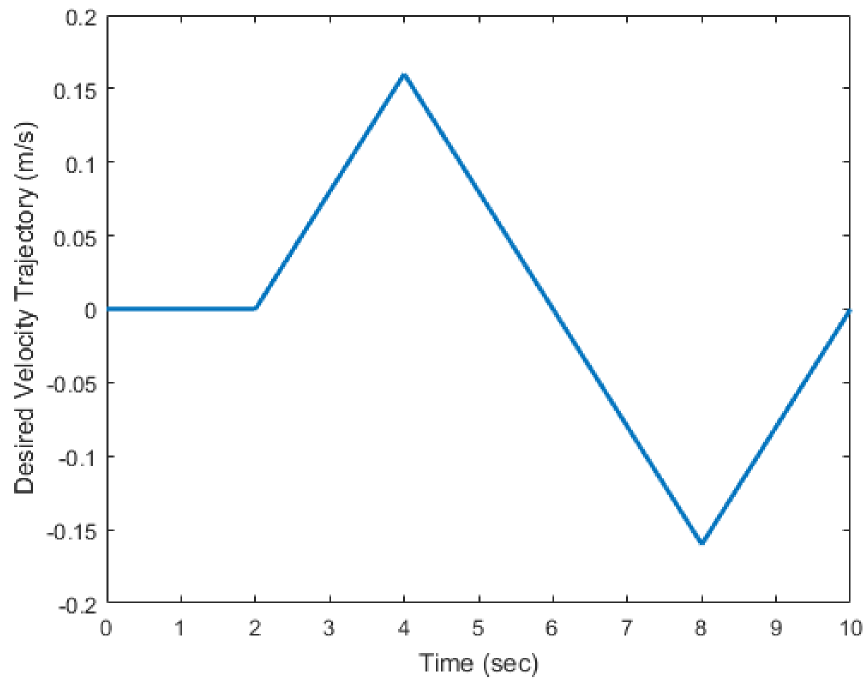

Figure 3. Desired EHA velocity trajectory.

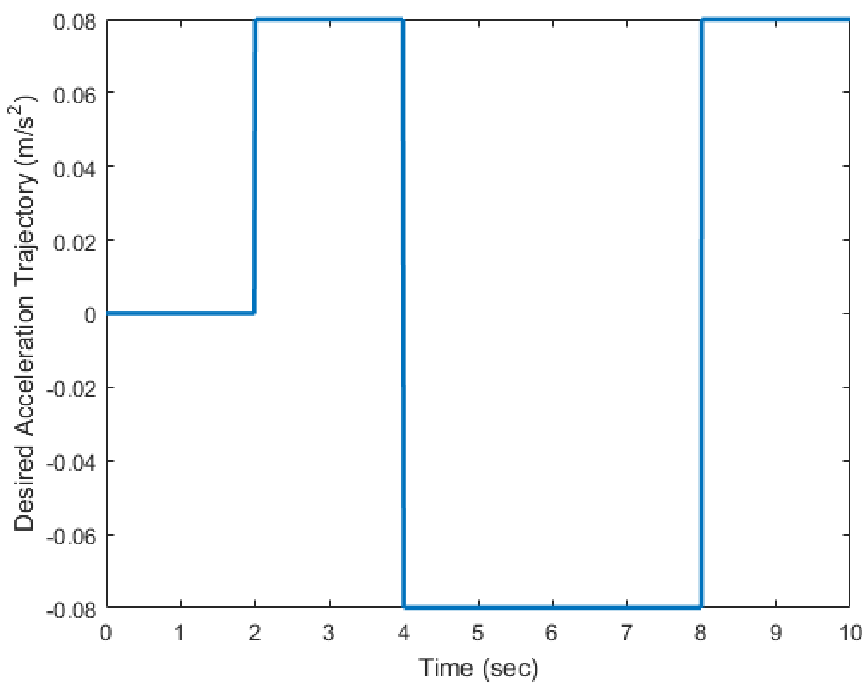

Figure 4. Desired EHA acceleration trajectory.

Note that for the first 4 seconds, the system behaved normally. A friction fault was injected at 4 seconds and lasted for 4 seconds. At 8 seconds, the friction fault was remove and a 2 second leakage fault was implemented.

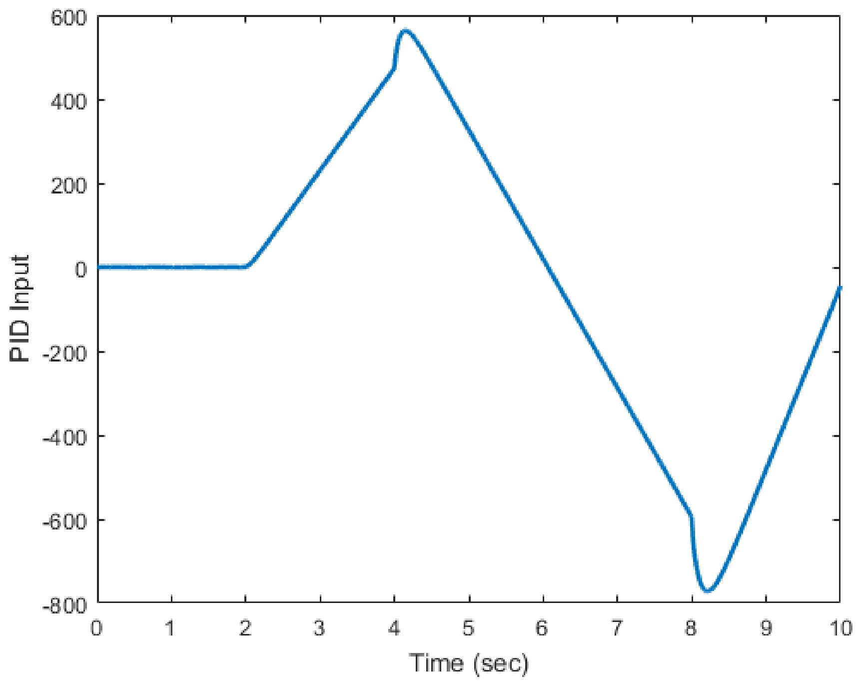

Figure 5. Calculated system input from PID controller.

Estimation and Fault Detection Results

The following three figures (Figs. 6-8) show the results of applying the KF and SVSF estimation strategies on the aforementioned electromechanical system. The estimation results for the KF and SVSF were nearly identical for the first two states. However, for the third state, the KF estimate was slightly noisier, whereas the SVSF smoothed out the estimated acceleration.

Figure 9 illustrates the acceleration state boundary layer values for each mode of operation. Recall that the system behaved normally for the first four seconds (A_1), followed by a four second friction fault (A_2), and finally a two second leakage fault (A_3). The magnitude of the calculated boundary layer, based on the SVSF gain and state error covariance matrix, provides a method for detecting system changes. A small magnitude indicates that the system behaviour closely matches the model used by the SVSF. Therefore, the Psi_{A_1} term is expected to be smaller than the other two boundary layer terms for the first four seconds, and is verified in Fig. 9. During the next four sections, the system operates in the presence of a friction fault (A_2), and the Psi_{A_2} term is found to be the smallest of the three. Finally, the system operates with leakage (A_3), and is verified since the magnitude of the Psi_{A_3} term is the smallest. The time-varying boundary layer that was derived in Section 3 is shown to be a viable term for fault detection and diagnosis. However, this method requires that the system behaves according to a finite number of models that the user or engineer can describe mathematically.

Another interesting property of the SVSF is observed when a spectrogram of the acceleration boundary layer values is created for each three modes of operations (Figs. 10-12). A spectrogram is a visual representation of the spectrum of frequencies in a signal as they vary with time or some other variable. In this case, the signal is based on the calculated time-varying boundary layer. Visual patterns appear in each figure based on the ratio of power and frequency (dB/Hz). Similar to the study of the boundary layer magnitudes, in this case, the smaller the ratio the better match in terms of system operation and the model used by the SVSF.

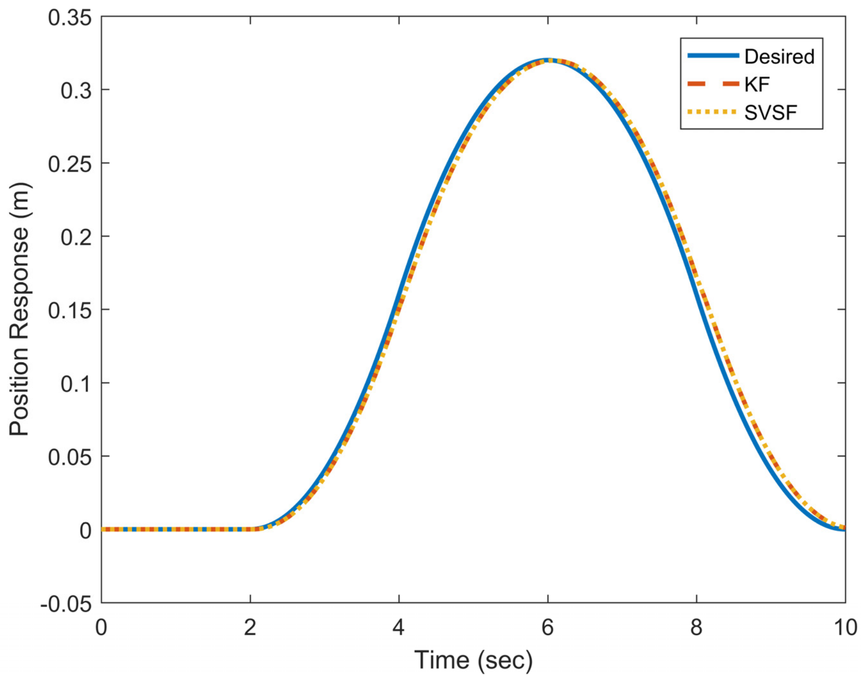

Figure 6. Estimated position trajectory using the KF and SVSF strategies.

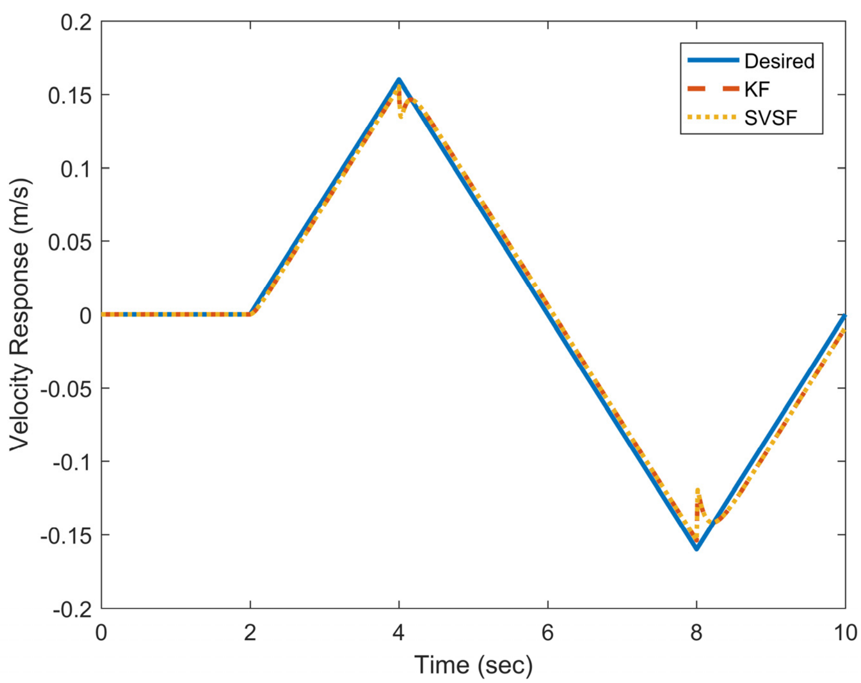

Figure 7. Estimated velocity trajectory using the KF and SVSF strategies.

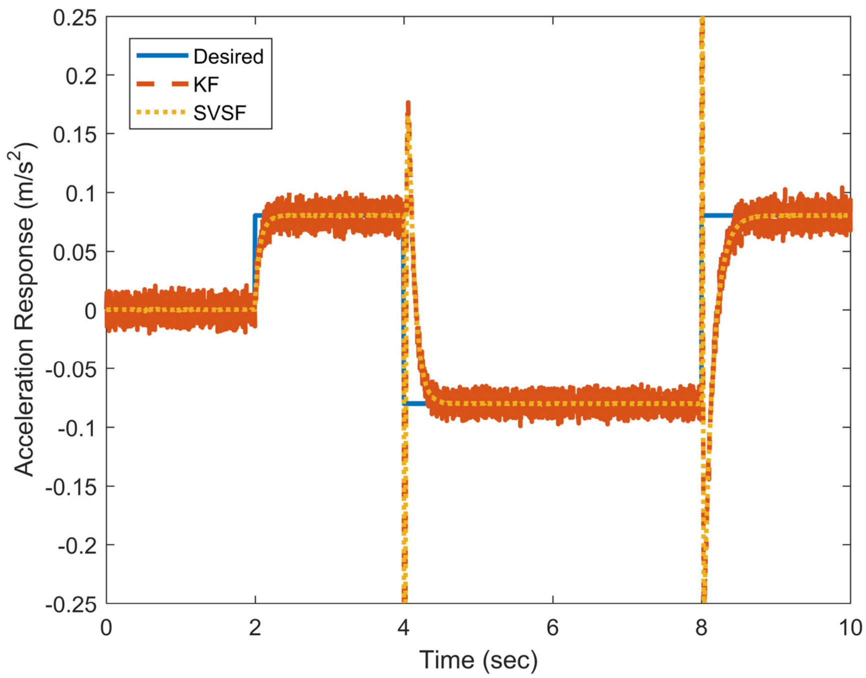

Figure 8. Estimated acceleration trajectory using the KF and SVSF strategies.

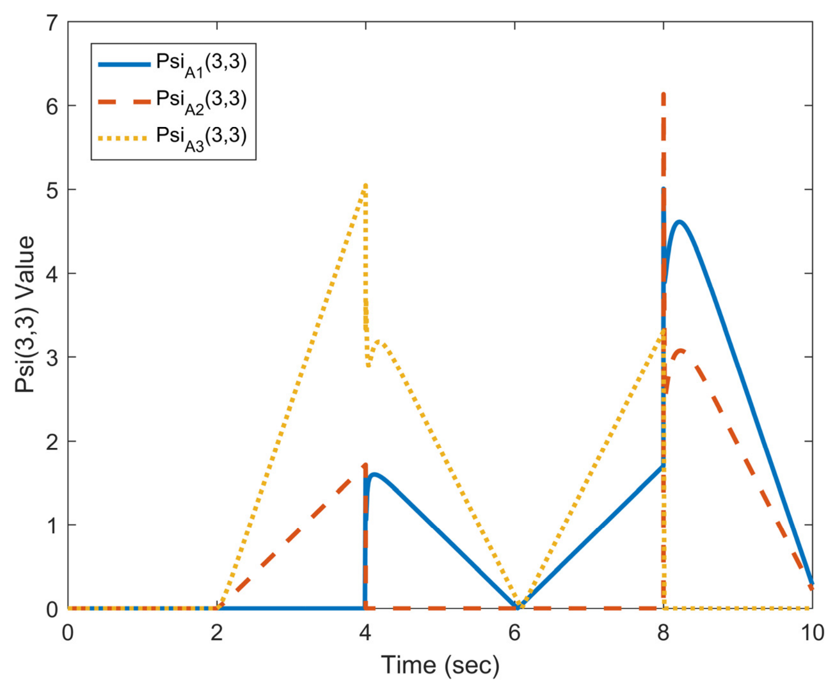

Figure 9. Acceleration state boundary layer values for each mode of operation.

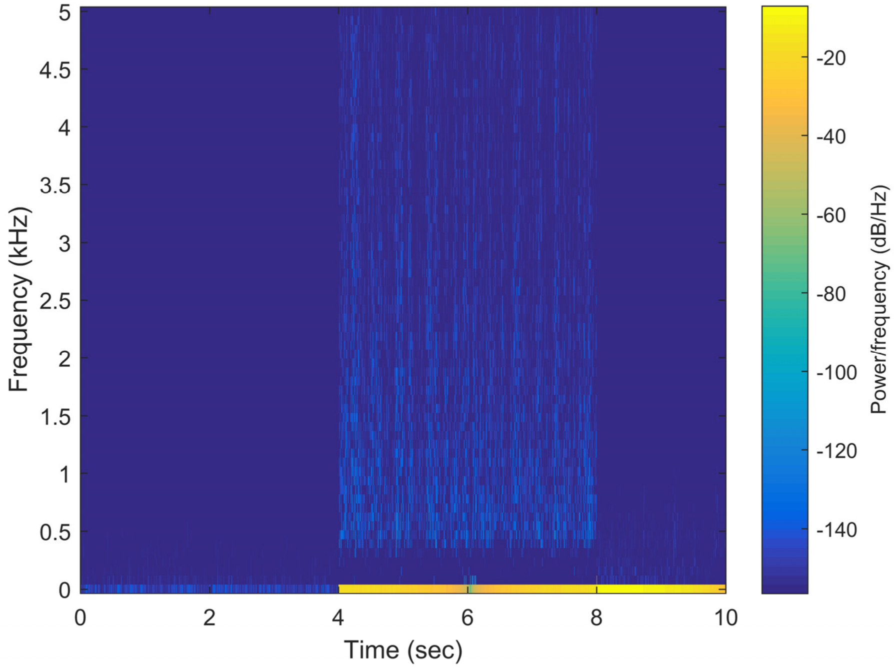

Figure 10. Spectrogram of the acceleration boundary layer values using the normal system model.

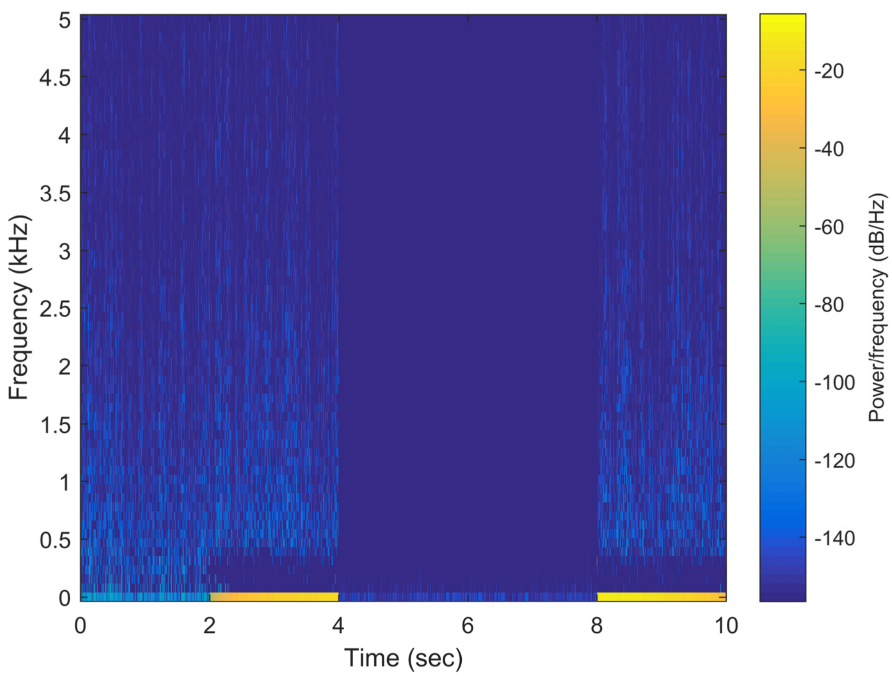

Figure 11. Spectrogram of the acceleration boundary layer values using the friction fault model.

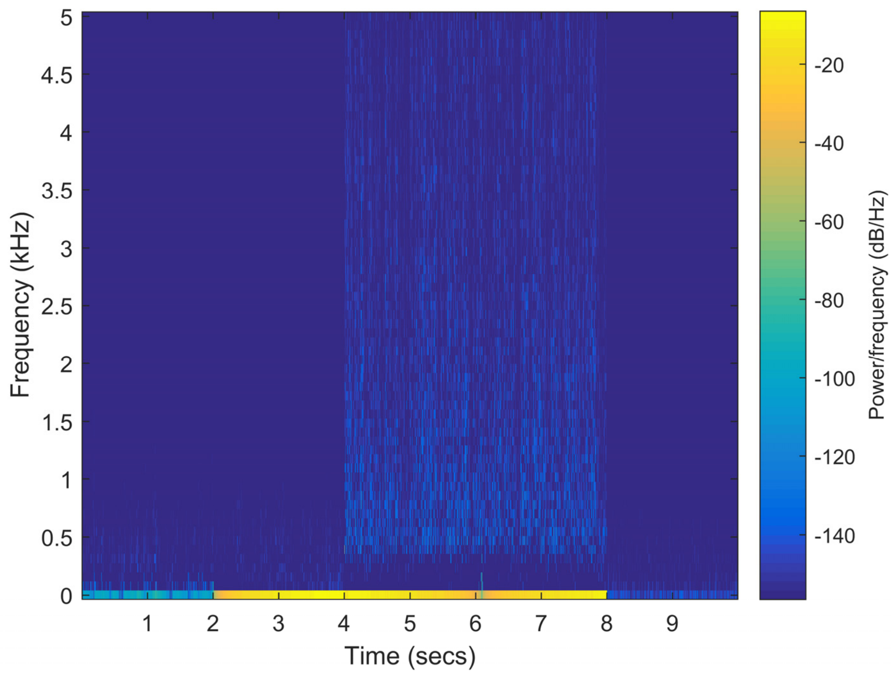

Figure 12. Spectrogram of the acceleration boundary layer values using the leakage fault model.

Figure 13 is a combination of Figs. 10-12 at low frequencies (less than 35 Hz). This figure clearly shows the presence of faults (low vs high power and frequency ratio). Based on knowledge of the system, the correct operating mode can easily be identified. For example, as per Psi_{A_1}, the system is shown to operate normally for four seconds, and then abnormally for the remainder of the simulation. The leakage fault (A_3) is shown to exist between 8 and 10 seconds, as per Psi_{A_3}.

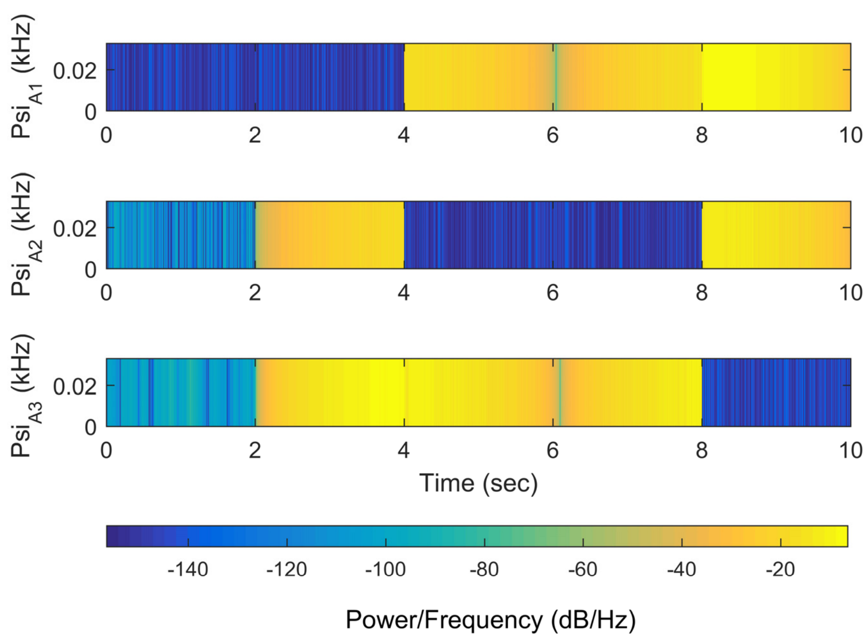

Figure 13. Low frequency spectrogram of the acceleration boundary layers for all three models.

5. CONCLUSIONS

Although first introduced in the 1950s, the most popular method used for signal processing and state estimation remains the Kalman filter (KF). The KF offers an optimal solution to the estimation problem under strict assumptions, however is known to be unstable due to modeling uncertainties and disturbances. The smooth variable structure filter (SVSF) is a sub-optimal filter but is considerably more robust than the KF. In this paper, properties of the SVSF were explored in an effort to detect and diagnosis faults in an electromechanical system. It was determined that the definition for the time-varying smoothing boundary layer may be used to accurately and quickly detect and identify changes in a system. Future work includes application of the proposed methodology to an experimental setup, and comparison of the results with other popular fault detection strategies.

6. REFERENCES

[1] N. Nise, Control Systems Engineering, 4 ed., New York: John Wiley and Sons, Inc., 2004.

[2] R. E. Kalman, "A New Approach to Linear Filtering and Prediction Problems," *Journal of Basic Engineering, Transactions of ASME,* vol. 82, pp. 35-45, 1960.

[3] B. D. O. Anderson and J. B. Moore, Optimal Filtering, Englewood Cliffs, NJ: Prentice-Hall, 1979.

[4] D. Simon, Optimal State Estimation: Kalman, H-Infinity, and Nonlinear Approaches, Wiley-Interscience, 2006.

[5] Y. Bar-Shalom, X. Rong Li and T. Kirubarajan, Estimation with Applications to Tracking and Navigation, New York: John Wiley and Sons, Inc., 2001.

[6] S. J. Julier, J. K. Ulhmann and H. F. Durrant-Whyte, "A New Method for Nonlinear Transformation of Means and Covariances in Filters and Estimators," *IEEE Transactions on Automatic Control,* vol. 45, pp. 472-482, March 2000.

[7] M. S. Grewal and A. P. Andrews, Kalman Filtering: Theory and Practice Using MATLAB, 3 ed., New York: John Wiley and Sons, Inc., 2008.

[8] P. Kaminski, A. Bryson and S. Schmidt, "Discrete Square Root Filtering: A Survey of Current Techniques," *IEEE Transactions on Automatic Control,* 1971.

[9] S. Hammarling, "A Survey of Numerical Aspects of Plane Rotations," 1977.

[10] H. Wang and R. Gregory, "On the Reduction of an Arbitrary Real Square Matrix to Tridiagonal Form," *Mathematics of Computation,* vol. 18, no. 87, pp. 501-505, 1964.

[11] J. Chandrasekar, I. S. Kim, D. S. Bernstein and A. J. Ridley, "Cholesky-Based Reduced-Rank Kalman Filtering," *Proceedings of American Control Conference (ACC),* pp. 3987-3992, 2008.

[12] H. H. Afshari, S. A. Gadsden and S. R. Habibi, "Gaussian Filters for Parameter and State Estimation: A General Review and Recent Trends," *Signal Processing,* vol. 135, pp. 218-238, 2017.

[13] V. I. Utkin, "Variable Structure Systems With Sliding Mode: A Survey," *IEEE Transactions on Automatic Control,* vol. 22, pp. 212-222, 1977.

[14] V. I. Utkin, Sliding Mode and Their Application in Variable Structure Systems, English Translation ed., Mir Publication, 1978.

[15] J. J. Slotine and W. Li, Applied Nonlinear Control, Englewood Cliffs, NJ: Prentice-Hall, 1991.

[16] M. V. Basin, A. Ferreira and L. Fridman, "Sliding Mode Identification and Control for Linear Uncertain Stochastic Systems," *International Journal of Systems Science,* pp. 861-869, 2007.

[17] S. K. Spurgeon, "Sliding Mode Observers: A Survey," *International Journal of Systems Science,* pp. 751-764, 2008.

[18] B. Ristic, S. Arulampalam and N. Gordon, Beyond the Kalman Filter: Particle Filters for Tracking Applications, Boston: Artech House, 2004.

[19] S. Haykin, Kalman Filtering and Neural Networks, New York: John Wiley and Sons, Inc., 2001.

[20] S. A. Gadsden, "Smooth Variable Structure Filtering: Theory and Applications," McMaster University, Hamilton, Ontario, 2011.

[21] S. A. Gadsden, M. Al-Shabi and S. R. Habibi, "Estimation Strategies for the Condition Monitoring of a Battery System in a Hybrid Electric Vehicle," *ISRN Signal Processing,* 2011.

[22] A. Gelb, Applied Optimal Estimation, Cambridge, MA: MIT Press, 1974.

[23] G. Welch and G. Bishop, "An Introduction to the Kalman Filter," 2006.

[24] S. R. Habibi and R. Burton, "The Variable Structure Filter," *Journal of Dynamic Systems, Measurement, and Control (ASME),* vol. 125, pp. 287-293, September 2003.

[25] S. R. Habibi and R. Burton, "Parameter Identification for a High Performance Hydrostatic Actuation System using the Variable Structure Filter Concept," *ASME Journal of Dynamic Systems, Measurement, and Control,* 2007.

[26] S. A. Gadsden, Y. Song and S. R. Habibi, "Novel Model-Based Estimators for the Purposes of Fault Detection and Diagnosis," *IEEE/ASME Transactions on Mechatronics,* vol. 18, no. 4, 2013.

[27] S. A. Gadsden, M. Al-Shabi, I. Arasaratnam and S. R. Habibi, "Combined Cubature Kalman and Smooth Variable Structure Filtering: A Robust Estimation Strategy," *Signal Processing,* vol. 96, no. B, pp. 290-299, 2014.

[28] S. A. Gadsden and A. S. Lee, "Advances of the Smooth Variable Structure Filter: Square-Root and Two-Pass Formulations," *Journal of Applied Remote Sensing,* vol. 11, no. 1, pp. 1-19, 2017.

[29] S. A. Gadsden, S. R. Habibi and T. Kirubarajan, "Kalman and Smooth Variable Structure Filters for Robust Estimation," *IEEE Transactions on Aerospace and Electronic Systems,* vol. 50, no. 2, pp. 1038-1050, 2014.

[30] S. R. Habibi, "The Smooth Variable Structure Filter," *Proceedings of the IEEE,* vol. 95, no. 5, pp. 1026-1059, 2007.

[31] S. A. Gadsden, M. El Sayed and S. R. Habibi, "Derivation of an Optimal Boundary Layer Width for the Smooth Variable Structure Filter," in *American Control Conference*, San Francisco, CA, USA, 2011.

[32] S. A. Gadsden and S. R. Habibi, "A New Robust Filtering Strategy for Linear Systems," *ASME Journal of Dynamic Systems, Measurements and Control,* vol. 135, no. 1, January 2013.

[33] H. H. Afshari, S. A. Gadsden and S. R. Habibi, "Robust Fault Diagnosis of an Electro-Hydrostatic Actuator using the Novel Optimal Second-Order SVSF and IMM Strategy," *International Journal of Fluid Power,* vol. 15, no. 3, pp. 181-196, 2014.

[34] M. A. El Sayed, "Multiple Inner-Loop Control of an Electrohydrostatic Actuator," McMaster University, Hamilton, Ontario, 2012.